Revista Internacional de Métodos Numéricos para Cálculo y Diseño en Ingeniería

Dynamic Multi-Objective Collaborative Optimization of Cement Combined Grinding Based on Cooperative Game and Temporal Awareness

Dianyuan Ju[1], **Xiaoyu Ma**[1], **Rongfeng Zhang**[2,*], **Qiang Zhang**[3,*], **Xiaohong Wang**[3] **and Zhao Liu**[3]

[1]Shandong Provincial Key Laboratory of Preparation and Measurement of Building Materials, University of Jinan, Jinan, China

[2]School of Chemistry and Chemical Engineering, University of Jinan, Jinan, China

[3]School of Electrical Engineering, University of Jinan, Jinan, China

ABSTRACT

To address the multi-objective collaborative optimization of quality, energy consumption, and yield under dynamic conditions in the Portland cement combined grinding process, this paper proposes a novel algorithm, CGDS-LTL, based on cooperative game theory and temporal perception. First, a hybrid temporal model combining Linformer, TCN, and LSTM was developed to dynamically track process conditions in the Portland cement combined grinding process. Second, an optimization objective function was established, and a cooperative game theory framework was introduced to address the challenge of achieving multi-objective optimization, which could not be effectively solved with a single pareto-optimal solution. Meanwhile, volatility metrics were used to quantify the adjustment range of operational variables, allowing for the dynamic optimization of decision constraints. This approach mitigated the deviation of the pareto front from current decision settings caused by high population randomness, ultimately identifying the optimal solution for the multi-objective collaborative optimization problem. Finally, experiments using real production data from a Portland cement plant demonstrated that, compared with NSGA-II and C-TAEA, the proposed method improved the hypervolume indicator by 95% and 33.3%, respectively, indicating a more uniform solution distribution and better convergence. This demonstrated the interpretability and effectiveness of the proposed framework for dynamic multi-objective optimization in Portland cement combined grinding.

OPEN ACCESS

Received: 14/04/2026

Accepted: 21/05/2026

DOI
10.23967/j.rimni.2026.10.83781

Keywords:
Cement grinding
cooperative game theory
multi-objective optimization
Linformer

1 Introduction

Cement is a key material for infrastructure construction and an important pillar of the national economy. Cement grinding is a critical stage of cement production and directly affects product quality [1]. Currently, most Chinese cement plants maintain the 45 μm sieve residue of finished cement at no less than 5% to ensure product quality. Under increasing market pressure, enterprises also emphasize higher hourly production output to maintain efficiency while meeting quality requirements. In addition, cement grinding accounts for about 65% of the total power consumption in cement

*Correspondence: Rongfeng Zhang, Qiang Zhang (cse_zhangrf@ujn.edu.cn, ave_zhangq@ujn.edu.cn).

production. Under the dual-carbon background, reducing grinding energy consumption has become a major industry concern [2,3]. Existing studies mainly optimize production indicators by adjusting operational parameters to ensure cement quality [4,5]. However, the cement grinding process involves complex operating conditions and strong variable coupling. Improper parameter adjustment can cause process fluctuations and even system instability, affecting production stability. Therefore, optimization studies are needed to improve quality, reduce energy consumption, increase production, and maintain stable operation in cement grinding processes.

In recent years, optimization research on industrial grinding processes has made significant progress, providing a foundation for multi-objective collaborative optimization [6,7]. Wang et al. [8] proposed a hybrid evolutionary algorithm that combines the population balance model and the response surface method, establishing a multi-objective nonlinear programming model to enhance grinding efficiency. Hu et al. [9] developed a carbon emission evaluation and optimization model by integrating a speed-variation-based regulation function with the NSGA-II algorithm, effectively reducing carbon emissions and processing costs. However, existing optimization methods for cement grinding processes still face several challenges. First, cement grinding requires coordinated optimization of quality, energy consumption, and production output, while most existing studies focus on single-objective or partial-objective optimization. Second, the cement grinding process exhibits strong coupling and dynamic time-varying characteristics, yet existing studies show limited capability in handling coupling relationships among multiple variables [10].

To achieve dynamic multi-objective collaborative optimization of cement grinding, a dynamic time-series model must be established first. Early studies primarily employed mechanism-based models for industrial process modeling [11], but these models struggled to accurately represent the strongly coupled and nonlinear characteristics of cement grinding. With the development of machine learning and deep neural networks, data-driven methods have been widely applied to industrial grinding [12,13]. Compared with mechanism-based models, data-driven models can better extract information from large-scale industrial data [14]. Reference [15] combined machine learning with response surface methodology to optimize machining and energy efficiency for 8000 series aluminum alloys, enabling the prediction of specific energy consumption and energy use. Öztürk et al. [16] integrated experimental testing with machine learning to reduce energy consumption and surface roughness in slot milling of AISI 316 stainless steel. However, despite their flexibility and adaptability, current data-driven models still face challenges in cement grinding processes, including insufficient real-time performance and limited generalization capability.

Second, many researchers have improved optimization algorithms for industrial processes. Early studies applied metaheuristic algorithms to industrial optimization problems [17]. Later, NSGA-II improved search efficiency and solution quality through non-dominated sorting and crowding distance calculation, and was widely used in multi-objective optimization [18,19]. Hybrid methods combining neural networks with optimization algorithms further provided effective solutions for complex industrial optimization problems [20,21]. Cook et al. [22] developed an NN-GA integrated model for particleboard manufacturing, achieving a prediction accuracy of 92.7%. Wang et al. [23] combined NSGA-II with BPNN for industrial turbomachinery design, introducing boundary control and a coarse-to-fine strategy to reduce sample requirements and obtain Pareto solutions. Although these methods improved multi-objective optimization in complex industrial processes, most only passively provide Pareto solution sets without considering collaboration among objectives, still relying on expert experience for decision-making. Moreover, existing studies mainly focus on static conditions and insufficiently consider production stability requirements.

To address the challenges of dynamic multi-objective collaborative optimization in the cement grinding process, the present work centers on the cement combined grinding process and proposes a data-driven collaborative optimization framework. The framework first establishes a multi-objective time-series optimization model that considers product quality, characterized by the 45 μm sieve residue, unit energy consumption, and hourly production output. Subsequently, the CGDS-LTL algorithm is developed. In this algorithm, dynamic operating condition tracking and a dynamic decision variable search strategy are employed to adaptively adjust operational variables while stably ensuring product quality. This enables a dynamic optimal balance between energy consumption and production output.

The main contributions of this study are summarized as follows.

- A dynamic operating condition tracking strategy based on a Linformer-TCN-LSTM hybrid architecture is proposed for time-series modeling of the cement combined grinding process. Linformer with multi-head attention captures global dependencies with reduced computational complexity, while the temporal convolutional network (TCN) enhances local temporal feature extraction, and LSTM captures long-term dependencies. Based on this, a sliding time-series model is constructed to achieve dynamic operating condition tracking.
- For the multi-objective collaborative optimization of the cement combined grinding process under dynamic operating conditions, a dynamic decision variable search strategy based on the Nash bargaining solution is proposed. A cooperative game-theoretic framework is introduced to overcome the limitation of single Pareto solutions in three-dimensional collaborative optimization. Meanwhile, a fluctuation coefficient (FC) is used to quantify operational variable adjustments and dynamically constrain decision variable ranges, reducing Pareto front deviations caused by population randomness.

2 Optimize Problem Description

The purpose of cement grinding is to grind clinker, gypsum, and additives into cement products in specified proportions. This section takes the cement combined grinding process of a cement plant as the background. It analyzes the dynamic variations of operational variables in the process and identifies the variables related to product quality, energy consumption, and production output. Fig. 1 shows the process flow diagram of the cement combined grinding process. The process consists of two stages, pre-grinding and finish grinding, with a roller press and a ball mill serving as the core equipment, respectively. In the grinding process of the cement plant studied in this paper, no separator is installed after the ball mill.

The cement combined grinding process is a continuous production process characterized by strong coupling, time delay, and nonlinearity. To ensure the stability of the grinding process and reduce operator-induced variability, it is necessary to establish a multi-objective optimization algorithm for the cement combined grinding process, as shown in Fig. 2. To improve the adaptability of the algorithm, cement type and grinding aid dosage are incorporated as modeling features. In addition, the production process is assumed to operate without faults.

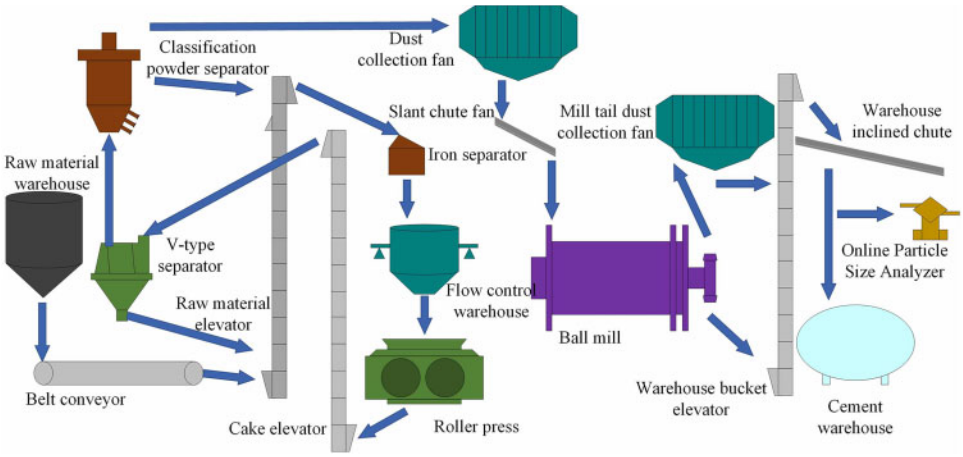

Figure 1: Open circuit grinding process of cement combined grinding

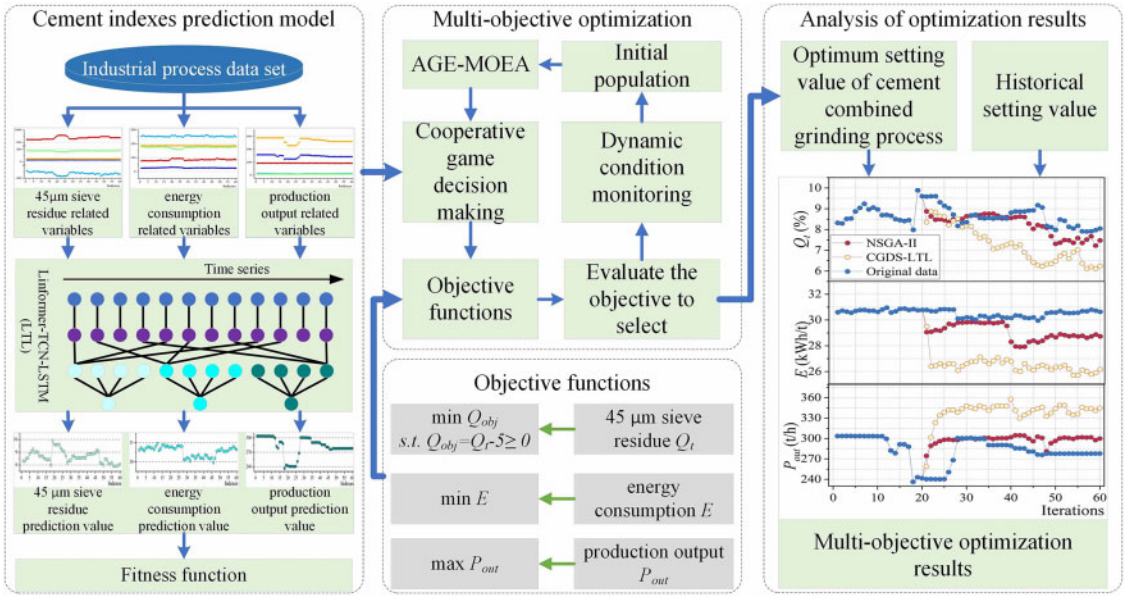

Figure 2: Optimization algorithm framework

2.1 Description of Cement Combined Grinding Process Model

2.1.1 Decision Variables

In this section, multiple operating variables are selected from the MES system of a Chinese cement plant as decision variables for the multi-objective optimization problem, as shown in Fig. 3. These variables are collected from high-precision sensors measuring temperature, pressure, current, and flow rate. Energy consumption data are obtained from smart meters, while particle size data are acquired from an online particle size analyzer. Since the analyzer is installed upstream of the cement silo, a time delay exists, and time alignment is required when constructing the time-series dataset. The delay, estimated at approximately 20 min based on material flow conditions and operator experience, is

identified using Cross-correlation Analysis to determine the maximum correlation lag between particle size and control variables. The time series is then shifted for alignment, and Cubic Spline Interpolation is applied to resample non-synchronous points, ensuring continuous and aligned timestamps and reducing the impact of delay on prediction accuracy.

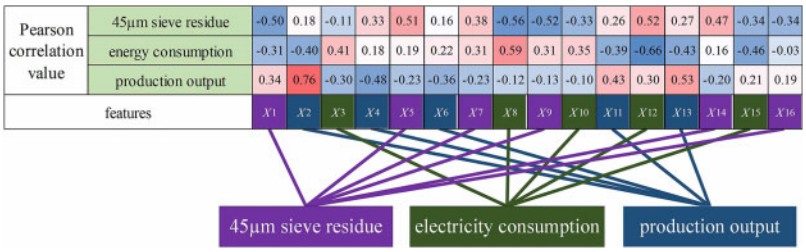

Figure 3: Relationship between operating variables and optimization objectives. The color bar on the right indicates the Pearson correlation coefficient, ranging from −1 (blue, negative correlation) to 1 (red, positive correlation)

The Pearson correlation analysis in Fig. 3 reveals that specific variables have varying influences on quality, power consumption, and production. However, because variables are tightly coupled in the cement grinding process, dividing them into independent subsets for different objectives would result in the loss of important system-level information. Thus, all variables from x_1 to x_{16} are combined as a global decision variable set X to capture system characteristics.

Based on the analysis of the cement combined grinding process shown in Fig. 1, the factors affecting the production indices include cement type (x_1), feed amount feedback value (x_2), steady flow bin weight (x_3), roller press movable roller side current (x_4), roller press fixed roller side current (x_5), roller press hydraulic pressure (x_6), V-type classifier inlet pressure (x_7), classifier powder separator current (x_8), classifier powder separator speed feedback (x_9), cake elevator current (x_{10}), grinding aid feedback value (x_{11}), ball mill current (x_{12}), internal pressure differential of the mill (x_{13}), ball mill outlet material temperature (x_{14}), high-concentration dust collector fan current (x_{15}), and high-concentration dust collector fan speed feedback (x_{16}). Fig. 3 presents the Pearson correlation coefficients and the relationships between the operating variables and the optimization objectives.

2.1.2 Feasibility Constraints

First, to ensure that cement quality meets the required standard, the 45 μm residue must satisfy the quality constraint specified as $Q_{obj} = Q_t - 5 \geq 0$, where Q_{obj} represents the target value of the 45 μm residue, and Q_t denotes the measured value obtained from the online particle size analyzer. In addition, to establish a multi-objective dynamic optimization model for the cement combined grinding process, the decision variables are constrained within specified ranges, and the corresponding boundary constraints are given in Table 1. The studied cement production line mainly produces three types of cement, P.O 42.5, P.O 52.5, and low-alkali P.O 52.5. Therefore, the value range of x_1 is set to 0–2.

Table 1: Bound constraints of decision variables

Variable	Name	Lower limit	Upper limit	Unit
x_1	Cement varieties	–	–	–
x_2	Feed amount feedback value	244.2	340.1	t/h
x_3	Steady flow bin weight	13.9	31.1	t
x_4	Roller press movable roller side current	19.6	55.3	A
x_5	Roller press fixed roller side current	30.2	47.4	A
x_6	Roller press hydraulic pressure	16.6	21.1	Mpa
x_7	V-type classifier inlet pressure	−470.8	−71.5	pa
x_8	Classifier powder separator current	127.1	272.7	A
x_9	Classifier powder separator speed feedback	795.9	1188.1	rpm
x_{10}	Cake elevator current	138.8	189.9	A
x_{11}	Grinding aid feedback value	399.7	625.3	t/h
x_{12}	Ball mill current	177.4	197.1	A
x_{13}	Internal pressure differential of the mill	145.7	421.1	pa
x_{14}	Ball mill outlet material temperature	64.5	73.1	°C
x_{15}	High-concentration dust collector fan current	57.2	95.1	A
x_{16}	High-concentration dust collector fan speed feedback	673.6	913.1	rpm

2.1.3 Objective Function

The multi-objective dynamic optimization objectives of the cement combined grinding process are denoted as G_1, G_2, and G_3, as defined in Eq. (1), corresponding to qualified cement quality, minimum energy consumption, and maximum throughput, respectively. Cement quality is ensured by constraining the 45 μm residue of the finished cement to be no less than 5%, as this proportion of fine particles improves the hydration rate and early strength of cement and is required by the latest relevant GB175 standard in China.

$$\begin{cases} G_1 = \min Q_{obj} = \min(Q_t\text{-}5) \\ G_2 = \min E \\ G_3 = \max P_{out} \end{cases} \tag{1}$$

In summary, the multi-objective dynamic optimization model for the cement combined grinding process is formulated in Eq. (2). Where G denotes the objective function, which aims to minimize the deviation between the 45 μm residue and 5%, minimize unit energy consumption, and maximize hourly throughput. In the constraint space of Eq. (2), f_1, f_2, and f_3 describe approximate nonlinear relationships modeled by a data-driven temporal model. X is the global decision variable set, $X = x_1, x_2, \ldots, x_{16}$. To avoid feature leakage and capture variable interactions, the full set X is used as input.

$$
\begin{aligned}
&G = \{\min Q_{obj}, \min E, \max P_{out}\} \\
&s.t.\ Q_{obj} = f_1(X) \\
&E = f_2(X) \\
&P_{out} = f_3(X) \\
&x_{imin} \le x_i \le x_{imax}
\end{aligned} \tag{2}
$$

Due to significant differences in physical units and numerical ranges among the optimization objectives, Z-score normalization is applied to preprocess the objective function values. This step eliminates unit effects and improves the reliability of the Nash equilibrium-based decision framework. This method transforms the data to a distribution with zero mean and unit standard deviation. It unifies the scales of multiple objectives and improves robustness to outliers in industrial data through the use of standard deviation. It also ensures balanced contributions of all participants in the game-based decision process.

3 Proposed Method

3.1 Dynamic Operating-Condition Tracking Strategy

By constructing a data-driven sliding temporal model, dynamic tracking of continuous production in the cement combined grinding process can be achieved. To tackle the multi-objective prediction requirements, a Linformer-TCN-LSTM (LTL) model is introduced. The overall model architecture is shown in Fig. 4. The input tensor of the model is denoted as $\mathbb{R}^{B\times C\times T}$, where $B = 1$ is the batch size, $C = 16$ is the number of feature variables, and $T = 20$ is the time window length. The output dimension is denoted as $\mathbb{R}^{B\times O}$, where $O = 3$ represents the predicted indicators of 45 μm sieve residue, energy consumption, and production.

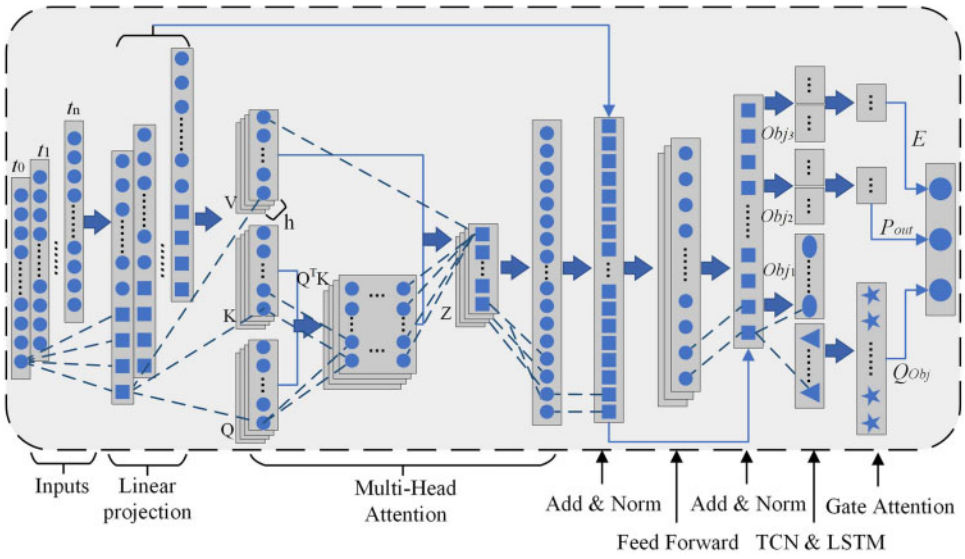

Figure 4: Linformer-TCN-LSTM model

To track operating conditions, a sliding-window scheme based on the LTL model is integrated, where Δt denotes the time interval. In a single optimization cycle, several consecutive historical data

points are selected and denoted as $0\sim t_1$. The dynamic decision-variable search strategy is then used to obtain the optimized decision variables at time t_2. These variables are fed into the LTL model to generate the operating-condition tracking result at time t_3, that is, the multi-objective prediction result. Here, the time intervals between t_1 and t_2 and between t_2 and t_3 are both Δt, whereas the interval from 0 to t_1 is not Δt. After each optimization is completed, the data window is shifted forward by one time interval Δt, and the optimization is performed again. The specific procedure is described in Eq. (3).

$$\begin{cases} y(t_3) = f(x(0), ..., x(t_1),\ x(t_2)) \\ y(t_4) = f(x(0+\Delta t), ..., x(t_1+\Delta t),\ x(t_2+\Delta t)), ... \\ y(t_n) = f(x(0+(n-3)\cdot\Delta t), ...,\ x(t_1+(n-3)\cdot\Delta t),\ x(t_2+(n-3)\cdot\Delta t)) \end{cases} \tag{3}$$

3.2 Dynamic Decision-Variable Search Strategy

This study proposes a dynamic decision-variable search strategy to address operating-condition instability in the cement combined grinding process that arises from excessive adjustments of operating variables. The strategy consists of FC calculation, cooperative game-based decision-making, and decision-variable space adjustment. The overall procedure is illustrated in Fig. 5.

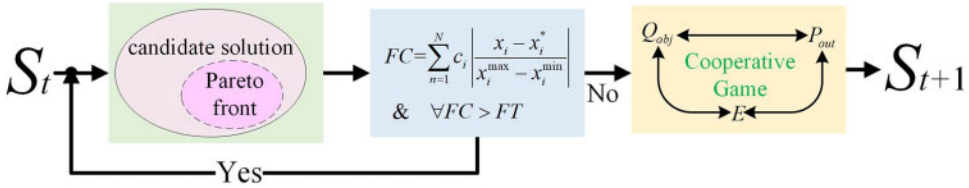

Figure 5: Dynamic decision-variable search strategy

3.2.1 Calculation of FC

The rationality of the decision-variable settings at the current time is evaluated by calculating the FC between the current settings and the subsequent settings, as shown in Eq. (4). The calculated FC is then compared with a predefined fluctuation thresholds (FT). If a solution satisfies the threshold requirement, the optimal cooperative solution is obtained through cooperative game-based decision-making. If none of the solutions meet the threshold requirement, the pareto front is recalculated by adjusting the decision-variable space, followed by repeated evaluation.

$$FC = \sum_{n=1}^{N} c_i \left| \frac{x_i - x_i^*}{x_i^{\max} - x_i^{\min}} \right| \tag{4}$$

where N denotes the total number of decision variables. $x_i^{\max}$ and $x_i^{\min}$ denote the upper and lower bounds of the i-th decision variable, respectively. x_i represents the corresponding pareto-front value of the i-th decision variable. x_i^* denotes the current setting of the decision variable. c_i represents the weight of the i-th decision variable. c_i is a process weighting factor that reflects the physical characteristics of each variable. This factor does not assign equal importance to all variables. It is initially determined based on the absolute values of the Pearson correlation coefficients and then fine-tuned with reference to operator experience. By introducing c_i, the fluctuation coefficient can more objectively represent the operational stability of the production process in physical terms. The value of FC ranges from 0 to 1. A smaller FC indicates a smaller adjustment magnitude of the decision variables and a more stable cement combined grinding process.

3.2.2 Cooperative Game-Based Decision-Making

In conventional multi-objective optimization, inherent conflicts exist among the objectives of qualified product quality, low energy consumption, and high production throughput. As a result, a single pareto-optimal solution is insufficient to satisfy the requirements of coordinated optimization in three or more dimensions. To address this decision-making dilemma, this article proposes a cooperative game-theoretic framework. In this framework, the three optimization objectives are modeled as rational collaborators, allowing multiple interests to be considered in a balanced manner.

The proposed cooperative game-theoretic framework first defines qualified cement quality (i.e., residue on the 45 μm sieve greater than 5%), minimization of energy consumption, and maximization of production throughput as game participants, denoted as P_Q, P_E, and P_P, respectively. The payoff function of each participant is constructed according to its corresponding physical objective. Together, these functions form a three-dimensional payoff space, as defined in Eq. (5). Where Q, P, and E denote the objective values of the pareto-optimal solutions. Q_{max}, P_{max}, and E_{max} represent the maximum values of each objective on the pareto front, while Q_{min}, P_{min}, and E_{min} denote the corresponding minimum values.

$$\begin{aligned} U_Q &= \begin{cases} 1 - \dfrac{Q-5}{Q_{\max}-5}, Q > 5 \\ 0, Q \le 5 \end{cases} \\ U_E &= 1 - \frac{E - E_{\min}}{E_{\max} - E_{\min}} \\ U_P &= \frac{P - P_{\min}}{P_{\max} - P_{\min}} \end{aligned} \tag{5}$$

The Nash product of each solution is calculated over the feasible solution set obtained after screening using the fluctuation coefficient. The threat point $d = [d_Q, d_E, d_P]$ is determined according to Eq. (6) by selecting the worst value of each objective within the feasible solution set. For each feasible solution, the product of the payoff gains of the three participants is computed according to Eq. (7). The solution that maximizes the Nash product is selected as the cooperative optimal solution. In addition, weighting factors can be introduced into each term of the Nash product according to practical production requirements. This allows a transition from absolute fairness to controllable fairness.

$$d_i = \min\{U_i(x) \,|x \in \text{pareto front}\}, i \in \{Q, P, E\} \tag{6}$$

$$\max \prod (U_i(x) - d_i), i \in \{Q, P, E\}$$

$$s.t. \tag{7}$$

$$x \in \text{pareto front}$$

$$U_Q(x) \ge d_Q, U_P(x) \ge d_P, U_E(x) \ge d_E$$

3.2.3 Decision-Variable Space Adjustment

The population generated by the optimization algorithm exhibits substantial randomness. This may cause the pareto front to deviate from the current settings of the decision variables. As a result, direct application to production could induce severe operating-condition fluctuations. Therefore, it

is necessary to dynamically adjust the bounds of each decision variable. When none of the pareto fronts satisfy the FT, the decision-variable space is adjusted, as formulated in Eq. (8). By modifying the constraint ranges of the decision variables, the pareto front is guided toward the current setpoints. This reduces the magnitude of decision-variable adjustments and mitigates fluctuations in the cement combined grinding process.

$$\begin{cases} x'_{i\min} = x_i^* - \left| x_{i\min} - x_i^* \right| * r \\ x'_{i\max} = x_i^* + \left| x_{i\max} - x_i^* \right| * r \end{cases} \tag{8}$$

where $x_{i\min}$ and $x_{i\max}$ denote the minimum and maximum values of the i-th decision variable, respectively. $x'_{i\min}$ and $x'_{i\max}$ represent the adjusted range of the variable. The parameter $r \in [0, 1]$ is the adjustment ratio and decreases with each optimization iteration. The adjustment of the variable space is performed with reference to the current setpoints of the decision variables. The constraint ranges are scaled by the ratio r.

In summary, the flowchart of the proposed algorithm is shown in Fig. 6.

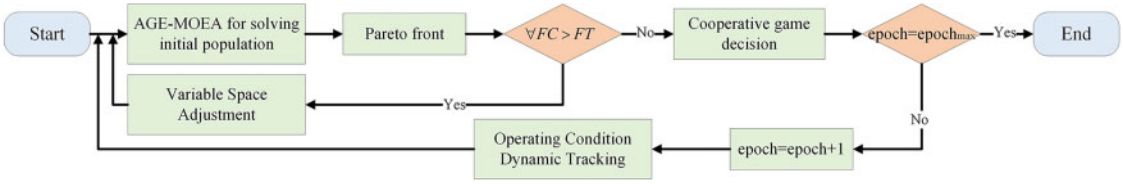

Figure 6: CGDS-LTL algorithm flowchart

4 Experiment

This section validated the effectiveness of the proposed algorithm through a series of experiments. All experimental data were obtained from the actual production process of a cement plant in China. The dataset was collected from the DCS and MES systems and included 16 decision variables and three objective variables. The experiments were conducted in a Python 3.9.19 environment using platforms including PyTorch 2.0.0. The models were trained on an RTX 5000 GPU with CUDA 11.7 support.

4.1 Performance Verification of LTL Temporal Model

To evaluate the multi-objective tracking accuracy and generalization ability of the proposed LTL temporal model, the method was compared with classical algorithms, including Random Forest (RF) and LightGBM, as well as widely used models such as Transformer-LSTM (TL) and TCN [24]. A sliding window approach was adopted. Considering the detection delay of the particle size analyzer and other factors, and in consultation with on-site operators, a time window of 20 min was used. This window was used to construct a dataset containing 60,260 time-series samples. The dataset was divided into training and test sets at a ratio of 9:1. For model training, the learning rate was set to 0.002. The mean squared error was used as the loss function, and the Adam optimizer was applied. The number of training epochs was set to 300. To prevent overfitting and improve model generalization, early stopping is used. 10% of the training data is held out as an independent validation set.

The training set was evenly divided into ten subsets. 10-fold cross-validation was then conducted for comparative experiments. The average results of the ten-fold cross-validation are shown in Table 2. The LTL model demonstrated good generalization ability. The TL model improved the R^2 values for power consumption and production by 2.11% and 1.04%, respectively. However, the increased

computational complexity of the Transformer led to a 2.38-fold increase in training time compared with the LTL model. This result indicated that Linformer reduces model complexity through low-rank attention and projection matrices. The TCN model had the shortest prediction time. However, its performance in multi-objective prediction was limited. The classical algorithms RF and LightGBM showed relatively poor performance in predicting the 45 μm sieve residue. RF had the longest training time, which was 5.16-fold that of the LTL model. Its prediction time was also not competitive. The performance of each model on the test set is shown in Fig. 7. The LTL model achieved the best regression performance for the 45 μm sieve residue. Its performance for power consumption and production was comparable to that of the TL model.

Table 2: Statistics of 10-fold CV results

Evaluation model	45 μm sieve residue (%)		Energy consumption (kWh/t)		Cement output (t/h)		Training time (s)	Prediction time (s)
	RMSE	R^2	RMSE	R^2	RMSE	R^2		
LTL	0.35	0.91	0.49	0.95	4.56	0.96	13.98	0.07
RF	0.37	0.86	0.53	0.93	4.98	0.92	86.17	0.65
LightGBM	0.39	0.87	0.51	0.94	4.72	0.93	27.82	0.34
TL	0.38	0.88	0.39	0.97	3.17	0.97	47.25	0.48
TCN	0.51	0.78	0.83	0.86	8.57	0.85	39.62	0.05

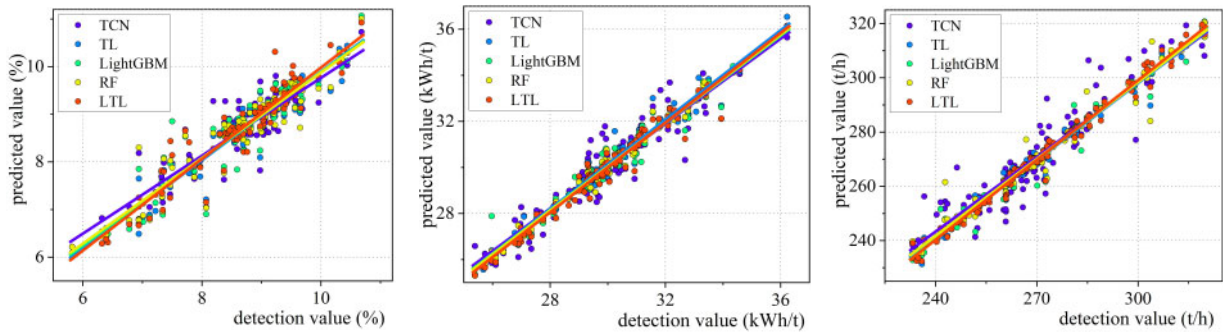

(a) 45μm sieve residue **(b)** Energy consumption **(c)** Cement output

Figure 7: Model prediction results

4.2 Comparison of Multi-Objective Optimization Algorithms

To verify the performance advantages of the CGDS-LTL algorithm in the multi-objective optimization of the cement combined grinding process, particularly its capability in handling dynamic time-varying processes, this section compared it with the C-TAEA and NSGA-II algorithms. Hypervolume (HV), Spacing (SP), and Spread were used as evaluation metrics. HV is used to measure the volume of the objective space dominated by the pareto solution set, reflecting both convergence and diversity. A larger HV value indicates better overall performance of the solution set. SP is used to evaluate the distribution uniformity of the pareto solution set. A smaller SP value indicates a more uniform distribution and better diversity. Spread is used to assess the extent and distribution uniformity of the

solution set. A smaller value indicates wider coverage and a more uniform distribution. The calculation procedures are given in Eqs. (9)–(11). Where S denotes the pareto set, $f_j(x_i)$ represents the i-th solution of the j-th objective value, and z^{ref} denotes the reference point. Before calculating the HV, the objective function values are linearly mapped to the interval [0, 1]. This mapping eliminates potential negative values after Z-score normalization and unifies the evaluation scale, where 1.0 represents the worst observed value. Based on this mapping, the reference point is set to 1.1 times the worst value, i.e., $z^{ref} = [1.1, 1.1, 1.1]$. This setting ensures that the HV metric is evaluated under a consistent and fixed reference framework. In addition, $\overline{d}$ is the average of d_i, and $d(e_k, S)$ denotes the minimum distance between the extreme solution of each objective and the solution set S. All optimization algorithms employed the LTL temporal model to evaluate the optimization process. The model parameter settings followed those in Section 4.1. The population size of each optimization algorithm was set to 30, and the number of generations was 100. For C-TAEA, the number of partitions was set to 10. Each algorithm was executed 25 times. The mean and variance statistics of the key performance indicators are summarized in Table 3.

$$HV = \text{volume}\left(\bigcup_{i=1}^{|S|}[f_1(x_i), z_1^{ref}] \times [f_2(x_i), z_2^{ref}] \times [f_3(x_i), z_3^{ref}]\right) \tag{9}$$

$$SP = \sqrt{\frac{1}{|S|-1}\sum_{i=1}^{|S|}(d_i - \overline{d})^2}, d_i = \min_{j\neq i}\sum_{k=1}^{3}\left|f_k(x_i) - f_k(x_j)\right| \tag{10}$$

$$Spread = \frac{\sum_{k=1}^{3} d(e_k, S) + \sum_{i=1}^{|S|}\left|d_i - \overline{d}\right|}{\sum_{k=1}^{3} d(e_k, S) + |S|\,\overline{d}} \tag{11}$$

Table 3: Statistics of different model metrics

Algorithm	HV		SP		Spread	
	Avg.	SD	Avg.	SD	Avg.	SD
CGDS-LTL	2.32	2.99	0.08	0.03	0.37	0.07
C-TAEA	1.19	1.60	0.11	0.05	0.80	0.10
NSGA-II	1.74	3.19	0.10	0.03	0.46	0.12

As shown in Table 3, the CGDS-LTL algorithm significantly outperforms the NSGA-II and C-TAEA methods across multiple performance metrics. The HV of CGDS-LTL increases by 95% and 33.3%, respectively. This indicates that the algorithm dynamically contracts the search boundaries through the variable-space adjustment mechanism, enhances local fine-grained search capability, and yields solution sets with improved convergence and overall quality. The SP values decrease by 27.3% and 20%, respectively. This demonstrates that the cooperative game-theoretic framework transforms multi-objective conflicts into a Nash bargaining problem, automatically identifies equilibrium solutions, and produces a more uniform distribution of the solution set. The Spread values decrease by 53.8% and 19.6%, respectively. This indicates that the algorithm constrains the adjustment magnitude of decision variables using the fluctuation coefficient. As a result, severe fluctuations in the production process are avoided, and the coverage of the solution set is improved. As illustrated by the optimization objective statistics of different algorithms in Fig. 8, CGDS-LTL maintains the residue on the 45 μm sieve at approximately 5%. At the same time, it achieves a significant reduction in energy consumption

and a steady increase in production throughput. This confirms its engineering value in dynamically optimizing energy consumption and production under the constraint of qualified product quality.

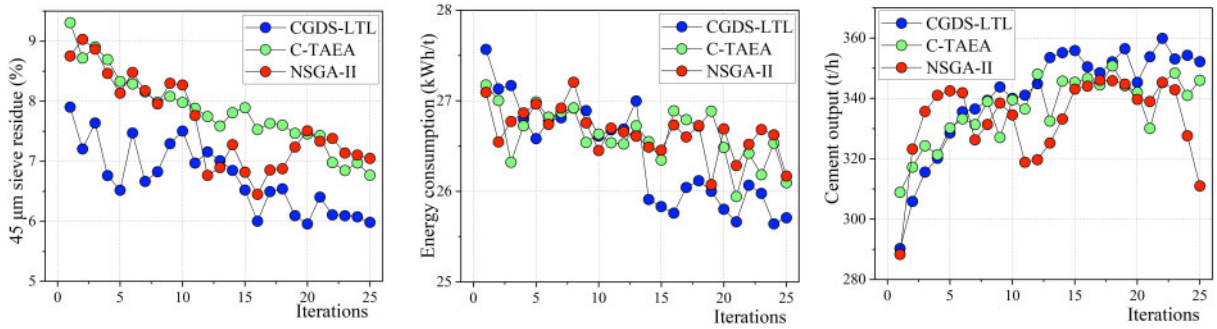

(a) 45 μm sieve residue **(b)** Energy consumption **(c)** Cement output

Figure 8: Comparison of optimization objective values for different models

4.3 Comparison of Multi-Objective Optimization Algorithms

In this section, different fluctuation thresholds, FT = 0.2, 0.25, 0.4, 0.6, and 0.9, were examined to identify the optimal configuration balancing convergence, diversity, and process stability. The algorithm settings were the same as those in Section 4.2. For each threshold, 25 optimization runs were performed. To reduce randomness, the algorithm was executed ten times for each FT value, and the results were averaged.

Taking x_{16} as an example, the box plots under different FT values are shown in Fig. 9. As FT decreased, the normal distribution curves and quartiles became more concentrated. When FT decreased from 0.9 to 0.25, data concentration increased by 30.8%, indicating that a smaller FT helps reduce operating-condition fluctuations. However, whether further reducing FT improves production performance still requires analysis with statistical performance indicators. When FT reached 0.25, the mean and quartile distributions changed little, while data concentration increased by only 5.9%. Therefore, further reduction of FT should be determined by overall production performance indicators.

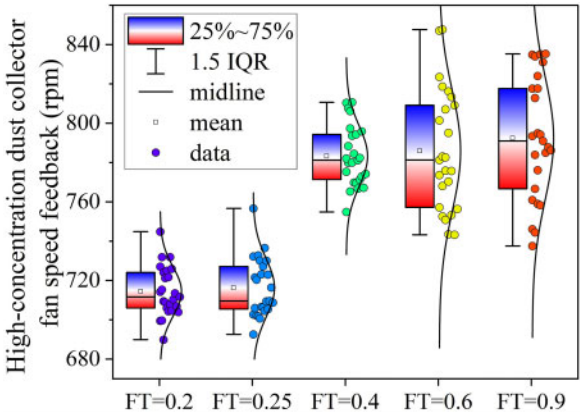

Figure 9: Statistical distribution of different FT decision variables

The statistical results of the 45 μm sieve residue, energy consumption, and production throughput under different FT conditions are shown in Fig. 10. When FT was 0.9 or 0.6, the variable-space adjustment strategy was rarely used, and the optimal solution was mainly selected from the Pareto front through the cooperative game-theoretic decision mechanism, resulting in relatively poor production performance. When FT decreased to 0.4, the algorithm computed FC values and occasionally applied the variable-space adjustment strategy, improving production performance. When FT was further reduced to 0.25, the algorithm achieved lower energy consumption and higher production throughput while maintaining qualified product quality.

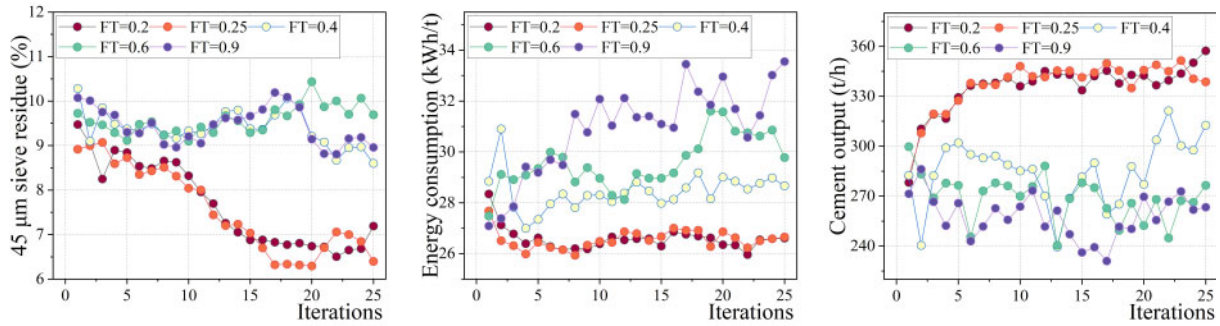

(a) 45 μm sieve residue **(b)** Energy consumption **(c)** Cement output

Figure 10: Comparison of optimization objective values for different FT

The statistical results of HV, SP, and Spread under different FT conditions are as follows. When FT = 0.9, the HV, SP, and Spread values are 0.88, 0.19, and 0.74, respectively. The relatively high FT value provides a larger solution space for the algorithm but leads to slower convergence. When FT was reduced to 0.4, HV increased by 90.9%, while SP and Spread decreased by 10.5% and 9.5%, respectively. This indicates that a moderate reduction in FT improves the search efficiency of the algorithm and reduces optimization bias. However, when FT was further reduced from 0.25 to 0.2, HV increased by only 0.8%, SP decreased by 0.1%, and the Spread value remained unchanged. This suggests that the effect of further reducing FT becomes saturated and that the balance between exploration and exploitation approaches its limit.

4.4 Industrial Data Analysis

In this section, one hour of real historical data from a cement combined grinding process was selected. The CGDS-LTL algorithm was applied to optimize the decision variables for the latter half of the time-series data. Its effectiveness was verified by comparing the resulting production indicators with those obtained using the original decision variables. To highlight the advantages of the proposed algorithm, the NSGA-II algorithm was also introduced for comparison. The parameter settings were consistent with those in Section 4.2. In this section, the FT value of the CGDS-LTL algorithm was set to 0.25. The comparative statistics of the production indicators are shown in Fig. 11.

Based on real historical operating data, the solution obtained using the CGDS-LTL algorithm yielded a 45 μm residue that was closer to the target value. The average power consumption was 29.87 kWh, representing a reduction of 2.18% compared with the historical power consumption. Meanwhile, the average hourly throughput reached 297.17 t/h, corresponding to an increase of 5.25%. In addition, compared with NSGA-II, the reduction in power consumption increased by 0.9%, the improvement in throughput increased by 2.87%, and the average FC value was reduced by 49.07. In summary, the

application of the CGDS-LTL algorithm reduced power consumption and increased hourly cement throughput while ensuring qualified product quality in the cement combined grinding process.

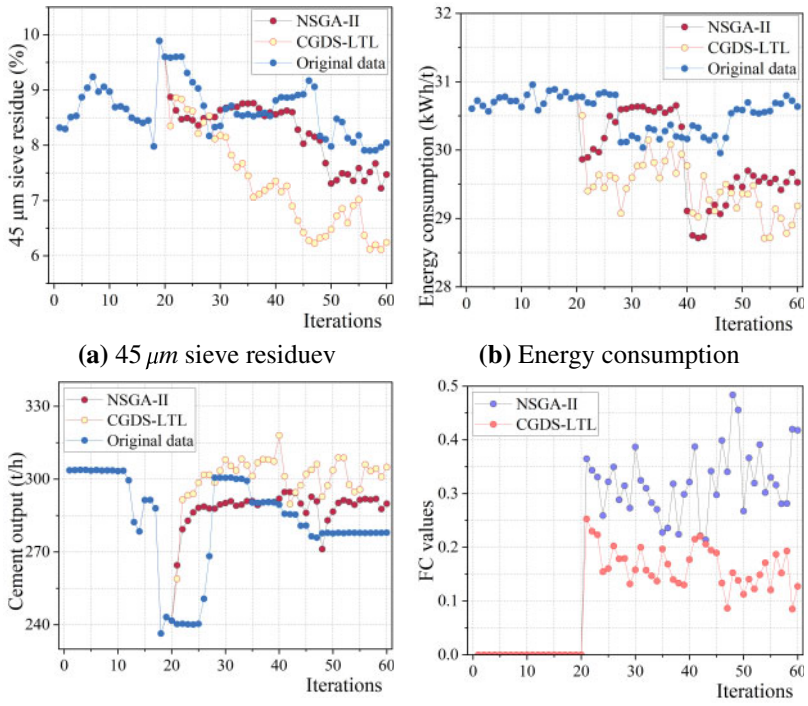

(a) 45 μm sieve residuev **(b)** Energy consumption

(c) Cement output **(d)** Comparison of FC values

Figure 11: Comparison of optimization objective value statistics

5 Conclusion

This study addressed the conflicts among multiple production indicators, the time-varying characteristics, and production stability issues caused by improper adjustment of operating variables in the cement combined grinding process. It proposed a dynamic multi-objective cooperative optimization algorithm (CGDS-LTL). The algorithm introduced a FC value to constrain the adjustment range of decision variables. It employed the Nash bargaining solution from cooperative game theory to achieve a multi-objective balance and incorporated a variable space adjustment strategy to enhance adaptability to time-varying operating conditions.

However, although the CGDS-LTL algorithm performed well, its adaptive capability in response to sudden process disturbances still requires validation. The current fluctuation threshold was set based on empirical tuning and lacks theoretical guidance. Future research will focus on developing an adaptive mechanism for the fluctuation constraint.

Acknowledgement: Not applicable.

Funding Statement: This work was supported by the University of Jinan Young Faculty Interdisciplinary Convergence Development Project 2025 (grant No. XKJC-202513), the University of Jinan Disciplinary Cross-Convergence Construction Project 2024 (grant No. XKJC-202408), the University

of Jinan Postdoctoral Research Start-up Fund Project (grant No. 100389909) and the Key Research and Development Plan of Shandong Province of China (grant No. 2024TSGC0559).

Author Contributions: The authors confirm contribution to the paper as follows: Conceptualization, Xiaohong Wang; methodology and writing—review, Rongfeng Zhang; experimental investigation and writing—original draft preparation, Dianyuan Ju; data curation, Xiaoyu Ma; formal analysis and method guidance, Qiang Zhang; funding acquisition and grammar correction, Zhao Liu. All authors reviewed and approved the final version of the manuscript.

Availability of Data and Materials: The data that support the findings of this study are available from the Corresponding Author, Rongfeng Zhang, upon reasonable request. The data used in this study were obtained from a cement enterprise and include key parameters such as product quality and production indicators. For reasons of commercial confidentiality, public disclosure of these data and their acquisition by competing companies could lead to unfair commercial competition. In addition, when obtaining the data, the authors explicitly agreed to the enterprise's binding confidentiality requirements, which strictly prohibit any form of data disclosure; violation of these requirements would entail corresponding legal liabilities.

Ethics Approval: Not applicable.

Conflicts of Interest: The authors declare no conflicts of interest.

References

1. Yang X, Su M, Shi X, Hao X. Dynamic multi-objective optimization method of cement grinding process based on knowledge-guided logistic regression. Powder Technol. 2025;463:121142. doi:10.1016/j.powtec.2025.121142.
2. Madlool NA, Saidur R, Rahim NA, Kamalisarvestani M. An overview of energy savings measures for cement industries. Renew Sustain Energ Rev. 2013;19:18–29. doi:10.1016/j.rser.2012.10.046.
3. Atmaca A, Kanoglu M. Reducing energy consumption of a raw mill in cement industry. Energy. 2012;42(1):261–69. doi:10.1016/j.energy.2012.03.060.
4. Zhu M, Ji Y, Peng T, Sun L. Knowledge-guided multi-objective operation optimization strategy for grinding process considering uncertain disturbances. Appl Soft Comput. 2025;183:113702. doi:10.1016/j.asoc.2025.113702.
5. Huang R, Ma Y, Li H, Sun C, Liu J, Zhang S, et al. Operation parameters multi-objective optimization method of large vertical mill based on CFD-DPM. Adv Powder Technol. 2023;34(6):104014. doi:10.1016/j.apt.2023.104014.
6. Brinksmeier E, TÖnshoff HK, Czenkusch C, Heinzel C. Modelling and optimization of grinding processes. J Intell Manuf. 1998;9(4):303–14. doi:10.1023/A:1008908724050.
7. Mitra K, Gopinath R. Multiobjective optimization of an industrial grinding operation using elitist nondominated sorting genetic algorithm. Chem Eng Sci. 2004;59(2):385–96. doi:10.1016/j.ces.2003.09.036.
8. Wang X, Liu L, Duan L, Liao Q. Multi-objective optimization for an industrial grinding and classification process based on PBM and RSM. IEEE/CAA J Automatica Sinica. 2023;10(11):2124–35. doi:10.1109/JAS.2023.123333.
9. Hu M, Sun Y, Gong Q, Tian S, Wu Y. Multi-objective parameter optimization dynamic model of grinding processes for promoting low-carbon and low-cost production. Processes. 2019;8(1):3. doi:10.3390/pr8010003.

10. Hao X, Wang Z, Shan Z, Zhao Y. Prediction of electricity consumption in cement production: a time-varying delay deep belief network prediction method. Neural Comput Appl. 2019;31(11):7165–79. doi:10.1007/s00521-018-3540-z.
11. Miller JA, Bowman CT. Mechanism and modeling of nitrogen chemistry in combustion. Prog Energy Combust Sci. 1989;15(4):287–338. doi:10.1016/0360-1285(89)90017-8.
12. Lv L, Deng Z, Liu T, Li Z, Liu W. Intelligent technology in grinding process driven by data: a review. J Manuf Process. 2020;58:1039–51. doi:10.1016/j.jmapro.2020.09.018.
13. Dai W, Chai T, Yang SX. Data-driven optimization control for safety operation of hematite grinding process. IEEE Trans Ind Electron. 2014;62(5):2930–41. doi:10.1109/TIE.2014.2362093.
14. Inapakurthi RK, Miriyala SS, Mitra K. Recurrent neural networks based modelling of industrial grinding operation. Chem Eng Sci. 2020;219:115585. doi:10.1016/j.ces.2020.115585.
15. Öztürk B, Küçük Ö, Aydın M, Kara F. Machine learning-guided energy-efficient machining of 8000 series aluminum alloys. Machines. 2025;13(10):906. doi:10.3390/machines13100906.
16. Öztürk B, Aydın K, Uğur L. Prediction of cutting performance in slot milling process of AISI 316 considering energy efficiency using experimental and machine learning methods. Multidiscip Model Mater Struct. 2025;21(4):850–66. doi:10.1108/MMMS-12-2024-0371.
17. Hopper E, Turton BCH. A review of the application of meta-heuristic algorithms to 2D strip packing problems. Artif Intell Rev. 2001;16(4):257–300. doi:10.1023/A:1012590107280.
18. Ma H, Zhang Y, Sun S, Liu T, Shan Y. A comprehensive survey on NSGA-II for multi-objective optimization and applications. Artif Intell Rev. 2023;56(12):15217–70. doi:10.1007/s10462-023-10526-z.
19. Zhang P, Qian Y, Qian Q. Multi-objective optimization for materials design with improved NSGA-II. Mater Today Commun. 2021;28:102709. doi:10.1016/j.mtcomm.2021.102709.
20. Nascimento CAO, Giudici R, Guardani R. Neural network based approach for optimization of industrial chemical processes. Comput Chem Eng. 2000;24(9–10):2303–14. doi:10.1016/S0098-1354(00)00587-1.
21. Chong HY, Yap HJ, Tan SC, Yap KS, Wong SY. Advances of metaheuristic algorithms in training neural networks for industrial applications. Soft Comput. 2021;25(16):11209–33. doi:10.1007/s00500-021-05886-z.
22. Cook DF, Ragsdale CT, Major RL. Combining a neural network with a genetic algorithm for process parameter optimization. Eng Appl Artif Intell. 2000;13(4):391–6. doi:10.1016/S0952-1976(00)00021-X.
23. Wang XD, Hirsch C, Kang S, Lacor C. Multi-objective optimization of turbomachinery using improved NSGA-II and approximation model. Comput Methods Appl Mech Eng. 2011;200(9–12):883–95. doi:10.1016/j.cma.2010.11.014.
24. Li X, Zhang L, Wang X, Liang B. Forecasting greenhouse air and soil temperatures: a multi-step time series approach employing attention-based LSTM network. Comput Electron Agric. 2024;217:108602. doi:10.1016/j.compag.2023.108602.